

Fitness Cost of Escape Mutations in p24 Gag in Association with Control of Human Immunodeficiency Virus Type 1

Javier Martinez-Picado,¹ Julia G. Prado,¹ Elizabeth E. Fry,² Katja Pfafferott,³ Alasdair Leslie,³ Senica Chetty,⁴ Christina Thobakgale,⁴ Isobel Honeyborne,³ Hayley Crawford,³ Philippa Matthews,³ Tilly Pillay,³ Christine Rousseau,⁵ James I. Mullins,⁵ Christian Brander,⁶ Bruce D. Walker,⁶ David I. Stuart,² Photini Kiepiela,⁴ and Philip Goulder^{3,6*}

irisiCaixa Foundation, University Hospital “Germans Trias i Pujol,” Barcelona, Spain¹; Division of Structural Biology, Henry Wellcome Building for Genomic Medicine, University of Oxford, Roosevelt Drive, Oxford OX3 7BN, United Kingdom²; Department of Paediatrics, Nuffield Department of Medicine, Peter Medawar Building for Pathogen Research, South Parks Road, Oxford OX1 3SY, United Kingdom³; HIV Pathogenesis Programme, The Doris Duke Medical Research Institute, University of Natal, Durban, South Africa⁴; Department of Microbiology, University of Washington, Seattle, Washington 98195⁵; and Partners AIDS Research Center, Massachusetts General Hospital, 13th Street, Building 149, Charlestown, Boston, Massachusetts 02129⁶

Received 15 October 2005/Accepted 9 December 2005

Mutational escape by human immunodeficiency virus (HIV) from cytotoxic T-lymphocyte (CTL) recognition is a major challenge for vaccine design. However, recent studies suggest that CTL escape may carry a sufficient cost to viral replicative capacity to facilitate subsequent immune control of a now attenuated virus. In order to examine how limitations can be imposed on viral escape, the epitope TSTLQEIQGW (TW10 [Gag residues 240 to 249]), presented by two HLA alleles associated with effective control of HIV, HLA-B*57 and -B*5801, was investigated. The *in vitro* experiments described here demonstrate that the dominant TW10 escape mutation, T242N, reduces viral replicative capacity. Structural analysis reveals that T242 plays a critical role in defining the start point and in stabilizing helix 6 within p24 Gag, ensuring that escape occurs at a significant cost. A very similar role is played by Thr-180, which is also an escape residue, but within a second p24 Gag epitope associated with immune control. Analysis of HIV type 1 *gag* in 206 B*57/5801-positive subjects reveals three principle alternative TW10-associated variants, and each is strongly linked to concomitant additional variants within p24 Gag, suggesting that functional constraints operate against their occurrence alone. The extreme conservation of p24 Gag and the predictable nature of escape variation resulting from these tight functional constraints indicate that p24 Gag may be a critical immunogen in vaccine design and suggest novel vaccination strategies to limit viral escape options from such epitopes.

Virus-specific cytotoxic T-lymphocyte (CTL) activity plays a central role in the control of immunodeficiency virus infection (18). Initial studies suggested that mutations resulting in a reduction of viral recognition by CTL—CTL escape—lead to diminished immune control (29). In certain instances, mutational escape has appeared to precipitate a rapid progression to AIDS (4, 19, 23). More recently, however, examples of CTL escape have been described for acute infections associated with subsequent successful control of viremia (11, 24, 26). In each case (22), and also in an example of escape occurring in chronic infection (12), reversion to the wild type was observed when the relevant viral mutant was transmitted to major histocompatibility complex-mismatched recipients. Reversion in the absence of the CTL-mediated pressure driving the selection of the escape mutant suggests a cost to viral replicative capacity incurred by acquisition of the relevant escape mutation. This was confirmed for examples from the simian immunodeficiency virus (SIV) macaque model (5, 11, 12, 13, 26) but

has yet to be demonstrated for human immunodeficiency virus type 1 (HIV-1) infection.

All examples published to date of reversion posttransmission are in epitopes within the capsid protein. Pressure for CTL escape in this conserved protein (34) is likely to be strongly opposed by selection pressure to resist amino acid sequence change. To better understand the mechanisms underlying effective control of HIV infection, we investigate here, in more detail, escape occurring within the p24 Gag epitope TSTLQEIQGW (TW10 [Gag residues 240 to 249]) that dominates the acute CTL response in individuals expressing HLA-B*57 or -B*5801 (2). These are the two HLA class I molecules independently associated with control of HIV-1 infection in South Africa (21). The commonest escape mutation, Thr→Asn at Gag-242 (T242N), reverts to Thr-242 following transmission to HLA-B*57/5801-negative individuals (24). The structural role of T242 within the capsid protein is described, and the consequences of the T242N mutation are evaluated. Three additional TW10 mutational escape options for HIV-1 are identified. In each case, the coexistence of additional, putative compensatory mutations is observed, indicating the extreme limitations on escape from this p24 Gag-specific response.

* Corresponding author. Mailing address: Peter Medawar Building, South Parks Rd., Oxford OX1 3SY, United Kingdom. Phone: 44-1865-281884. Fax: 44-1865-281236. E-mail: philip.goulder@ndm.ox.ac.uk.

MATERIALS AND METHODS

Study cohorts. The study cohorts used here have been previously described (24). The 258 C-clade-infected subjects analyzed in this study were collected from Durban, South Africa, and predominantly consisted of Zulu/Xhosa women recruited from the Cato Manor and St. Mary's Hospital, Mariannhill, South Africa, antenatal clinics. These subjects were all antiretroviral therapy (ART) naïve. The median viral load was 21,900 HIV RNA copies/ml plasma (range, <50 to 6.88×10^6), and the median absolute CD4 count was 449/mm³ (range, 101 to 1,215/mm³). The 187 B-clade-infected subjects were collected from diverse sources encompassing Europe, the Caribbean, and North America. Seventeen percent of these subjects were receiving ART at the time of analysis. The median viral load in those not receiving ART was 24,600 RNA copies/ml plasma (range, <400 to >750,000). The median CD4 count for those not receiving ART was 420/mm³ (range, 131 to 1,280/mm³).

Construction of p24 recombinant virus. Proviral DNA was extracted from peripheral blood mononuclear cells from an HLA-B57-negative child (SMH-05-Child) who had been vertically infected from his HLA-B57-positive mother (24). The sample corresponded to a sample with a mixture of Thr and Asn at Gag residue 242 (24). The p24 capsid coding region of *gag* was PCR amplified using the primers 5'-GAT AGA GGA AGA GCA AAA CAA A-3' (positions 1098 to 1119 in HIV-1_{HXB2}; a SapI restriction site is underlined) and 5'-TTT TTC CTA GGG GCC CT-3' (positions 2005 to 2021; an ApaI restriction site is underlined). The PCR fragment obtained was digested with SapI and ApaI and subcloned into plasmid p83-2 (17), which contains an HIV-1_{NL4-3} backbone. Two different clones were selected where the only difference was the presence of a threonine or an asparagine at Gag residue 242.

Site-directed mutagenesis. The T242N mutant virus was constructed in p83-2 by substituting Asn for Thr at Gag position 242 with the GeneTailor site-directed mutagenesis system (Invitrogen, Barcelona, Spain). The whole plasmid DNA was PCR amplified in a mutagenesis reaction with the following two overlapping primers, one of which contained the target mutation: p24/1497-1526, 5'-A GCA GGA ACT ACT AGT AAC CTT CAG GAA CA-3' (mutagenesis site is underlined); and p24/1497-1513, 5'-T ACT AGT AGT TCC TGC TAT GTC ACT TCC CC-3'. The presence of the T242N mutation was verified by DNA sequencing from nucleotide positions 983 to 1656 of Gag from newly generated plasmid clones. The DNA fragment ranging from the SapI site (position 1107) to the ApaI site (position 2010) was then subcloned into a new p83-2 plasmid to avoid carryover of potentially undesirable mutations in the mutagenized plasmid, and the p24 coding region sequence was verified again.

Generation of viral stocks. Viral stocks were generated in MT4 cells by electroporation with the mutant proviral plasmid carrying the 5' half of the genome (p83-2 and derived mutants) and a plasmid carrying the 3' half of the genome of HIV-1_{NL4-3} (p83-10). The 50% tissue culture infective dose was determined for each viral stock on MT4 cells, using the Spearman-Kärber method.

Single-cycle infectivity assay. The infectivity of viral stocks was measured by the single-cycle infectivity assay with Ghost-CXCR4 cells (17). Briefly, a total of 5×10^4 cells/well were infected in triplicate with 50 ng of p24 antigen equivalents of virus in the presence of 20 µg of Polybrene/ml by spin inoculation (3 h at $1,500 \times g$ and 22°C). The proportion of green fluorescent protein (GFP)-positive cells was measured by fluorescence-activated cell sorting analysis at 24 h postinfection.

Analysis of relative replicative fitness in virus mixtures. Growth competition assays were performed with MT4 cells as described elsewhere (17). Infections were initiated with unequal amounts of two competing virus variants, according to virus infectivity titrations, to a multiplicity of infection of 0.001. Unequal ratios were used based on the rationale that an increase in the proportion of the initially less abundant virus suggests a relatively better replicative capacity than that of the competing, initially more abundant virus, although random factors cannot be excluded with either unequal or equal starting ratios. Five-milliliter cultures were maintained in six-well tissue culture plates at 0.5×10^6 cells/ml. Every 3 to 4 days, MT4 cells were reinfected with a 1:100 dilution of the supernatant and cultured at 0.5×10^6 cells/ml.

Supernatants were removed from the cultures every 3 to 4 days for 60 days and were stored at -80°C. Viral RNAs were extracted from the supernatants (Qiamp RNA mini kit; QIAGEN) and PCR amplified in duplicate in two independent PCRs. The relative proportions of the two competing variants were determined at each passage based on the ratios of the specific mutations. Ratios were estimated based on the relative peak heights in electropherograms obtained by automated sequencing of HIV-1 p24 from culture supernatants. Genotyping was performed by using a BigDye Terminator cycle sequencing kit (Applied Biosystems) and subsequent electrophoresis in an automated sequencer (ABI PRISM

3100; Applied Biosystems). MT4 cells were also separately infected with mutants in the absence of wild-type virus to assess possible spontaneous reversion of the mutated codons.

Isolation, amplification, and sequencing of HIV-1 *gag*. Sequences for the 206 B*57/5801-positive and 239 B*57/5801-negative subjects were determined from proviral DNAs by population sequencing (24). All sequencing was carried out using BigDye V3 ready reaction termination mix (Applied Biosystems).

Statistical analysis. The identification of polymorphisms associated with the TW10 mutations identified at Gag positions 242, 248, 250, and 252 was undertaken using Fisher's exact test (see Fig. 3) for each of these four polymorphisms against all other polymorphisms in the N-terminal domain of p24 (residues 133 to 283), where the variation in B*57/5801-positive subjects was >10% of the consensus. These variations were at Gag positions 138, 146, 147, 163, 165, 215, 219, 223, 228, 256, and 260. Polymorphisms at Gag positions 146, 147, 163, and 165 are previously defined B*57/5801-associated CTL escape mutations (24, 25).

RESULTS

Dominance of T242N escape mutation. Initial studies of individuals expressing HLA-B*57 and -B*5801 described the early selection of escape mutations within the epitope TSTL QEIQGW (Gag residues 240 to 249), arising principally at residues 242 and 248. In an extended analysis to examine the alternative TW10 mutational escape strategies available to HIV-1, two large cohorts of B- and C-clade-infected persons were studied, including 206 B*57/5801-positive subjects (116 B*57-positive and 90 B*5801-positive subjects) (Table 1) and 239 B*57/5801-negative subjects. The T242N mutation arose in 74% (153/206) of B*57/5801-positive subjects. Substitutions at Gag residue 248, usually G248A, mainly arose in B clade infections (61% [49/80] of subjects) and arose in only a minority (15%) of C-clade-infected subjects, where Ala-248 was the consensus form.

T242N mutation reduces viral replicative capacity. The principal B*57/5801-TW10 escape mutation, T242N, is found transiently or not at all in B*57/5801-negative subjects, since transmission of this T242N variant to a B*57/5801-negative subject was followed by reversion to the wild-type residue T242 (24). In order to determine whether this implied cost of the T242N mutation to viral replicative capacity is observed in vitro, the replication of NL4-3 was compared in competition assays with that of a virus differing only in the T242N substitution (Fig. 1A). In addition, an NL4-3 virus containing the *gag* sequence obtained from a B*57-negative child in whom reversion to the wild-type residue T242 subsequently occurred was compared to a virus differing only in the T242N mutation (Fig. 1B). In each case, the wild-type virus outgrew the T242N variant. These data support the earlier inference of a fitness cost of the T242N mutation from observations of reversion in B*57/5801-negative subjects (24).

The extent of the reduced viral fitness due to the T242N mutation evident from in vitro competition experiments was not, however, consistently seen in single-cycle replication assays with GFP-expressing cells (Fig. 1C). This suggests that the T242N mutation does not cripple the virus but acts more subtly to partially disable it. These data are consistent with the observation that replacement of the T242N mutant virus by a T242-containing wild-type virus takes tens of months (24).

Structural role of T242. In order to understand the structural constraints on the Gag capsid, it is useful to consider the multiple roles of this polypeptide during the virus life cycle. The Gag capsid (CA; Gag residues 133 to 363) comprises two

TABLE 1. Patterns of sequence variation in HLA-B*57- and -B*5801-positive subjects within Gag epitope TW10 (residues 240 to 249) in B and C clade infections

Infection type and TW10 sequence	No. of subjects expressing allele			
	B*57	B*5801	B*57/5801	B*57/5801 negative
B clade				
TSTLQEQIGW (consensus)				
-----	6	0	6	71
--N-----	19	5	24	1
--N-A---A-	1	0	1	0
--N-----A-	25	5	30	1
--N-----T-	3	1	4	0
--N-----Q-	3	0	3	0
--N-S---A-	1	0	1	0
--N---VA-	1	0	1	0
-TN-----A-	1	0	1	0
---H---A-	1	0	1	0
-----A-	5	1	6	17
-----D-	1	0	1	0
----P-----	1	0	1	0
Other	0	0	0	17
Total	68	12	80	107
C clade				
TSTLQEQIAW (consensus)				
-----	1	18	19	107
--N-----	24	44	68	2
--N-A-----	3	0	3	0
--N-G-----	1	0	1	0
--N-----T-	6	3	9	0
--N-----V-	3	0	3	0
--N-----G-	0	1	1	0
--N-----N-	2	1	3	0
--S-----	0	2	2	4
---P-----	0	5	5	0
---T-----	1	0	1	0
---P---G-	0	1	1	0
---A-----	0	2	2	0
-----MT-	1	0	1	0
-----LD-	1	0	1	1
-----D-	1	0	1	0
-----Q-	1	1	2	1
-----I--	1	0	1	0
-----V--	1	0	1	3
-----M--	1	0	1	0
Other	0	0	0	14
Total	48	78	126	132

predominantly α -helical domains, i.e., an N-terminal (CA^N ; residues 133 to 283) and a C-terminal (residues 284 to 363) domain. The B*57/5801-TW10 epitope (Gag residues 240 to 249) thus lies within the N-terminal domain. Following cleavage of Gag matrix (MA; Gag residues 1 to 132), the capsid rearranges into the characteristic cone-shaped core structure packaging the RNA genome within the virion. The N terminus of CA^N (Fig. 2) forms a beta-hairpin structure subsequent to Gag cleavage, triggering capsid assembly via the formation of a salt bridge between the new N-terminal amide group and a buried carboxyl group (Asp-183). CA^N is also responsible for packaging copies of the host protein cyclophilin A (CypA; a prolyl isomerase and chaperone protein), which is essential for HIV infectivity (8).

Structures are available for mature CA^N (7, 28), immature CA^N (a construct incorporating MA) (31), and a complex of

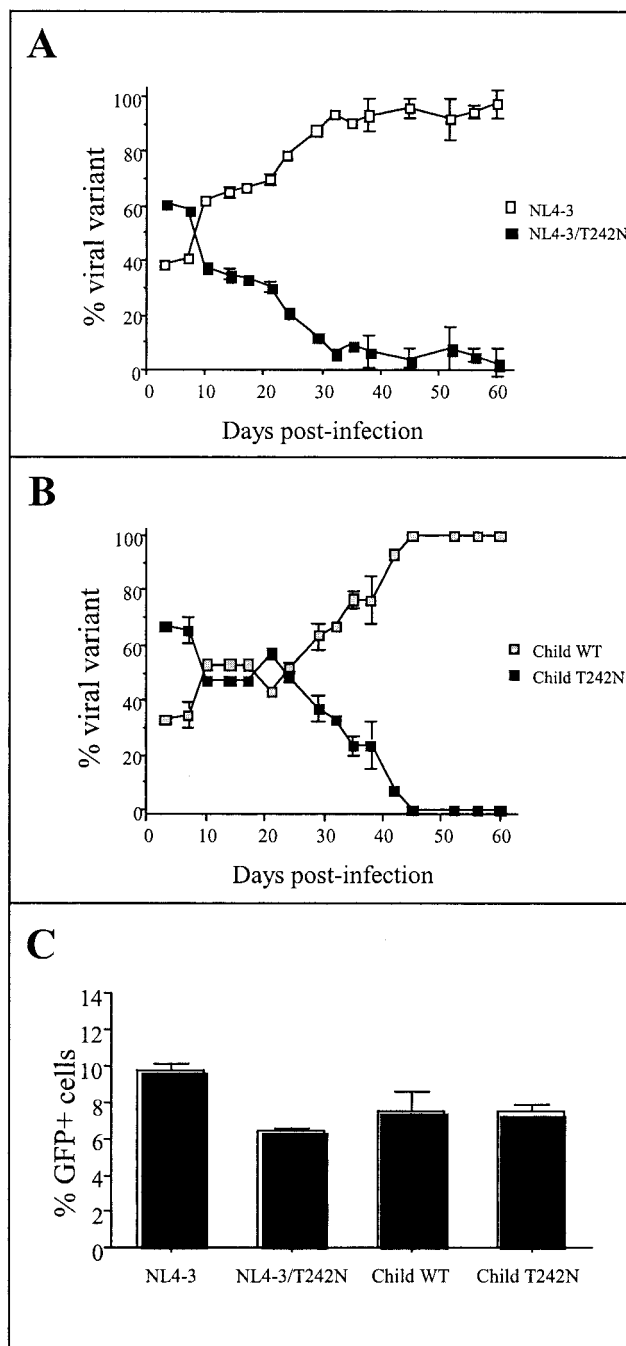


FIG. 1. Fitness cost resulting from T242N mutation. (A) Competition experiments in MT4 cells between HIV-1_{NL4-3} and its site-directed T242N mutant. (B) Competition experiments in MT4 cells between p24 recombinant viruses from an HLA-B*57-negative child (SMH-05-Child) who was vertically infected by his HLA-B*57-positive mother. The only difference between both viral recombinants is the presence of Thr or Asn at Gag residue 242. (C) Infectivities of individual viral isolates, as assessed with Ghost reporter cells. The rate of infectivity is expressed as the percentage of GFP-positive cells at 24 h postinfection. The results shown represent the means \pm standard deviations from two experiments.

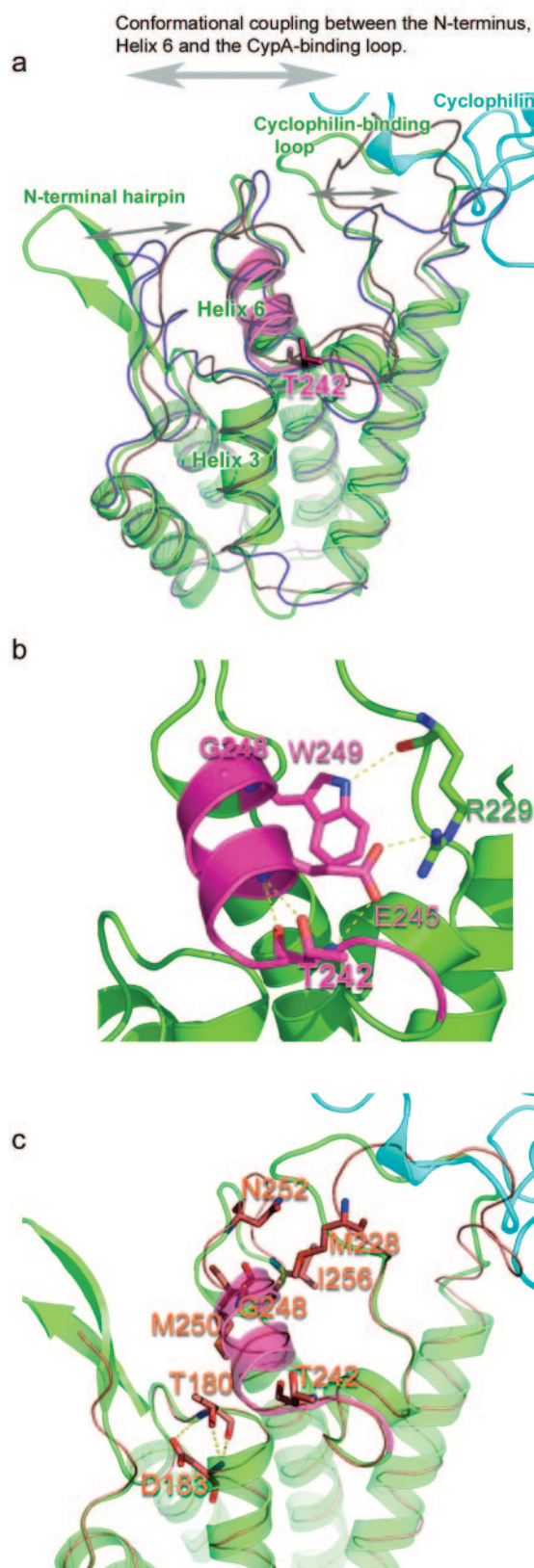


FIG. 2. Structural basis for fitness cost of T242N mutation. (a) Superimposition of capsid N-terminal domain structures. Gray rope, immature capsid structure (6, 31); purple rope, mature capsid struc-

ture (6, 31); green ribbon, CypA-bound structure (6, 14); cyan ribbon, CypA. Gray arrows indicate the observed conformational movements in the N-terminal hairpin, the CypA binding loop, and helix 6. Residue T242 is shown in magenta and drawn in stick representation. (b) Close-up of the TW10 epitope (magenta). The T(242)XXE(245) N-terminal cap for helix 6 is shown, with hydrogen bonds drawn as yellow dashes. Side chains (6) are drawn in stick representation. Hydrogen bonds between Trp-249, Glu-245, and the base of the CypA loop are shown together with Gly-248. (c) Ribbon representation as in panels a and b, with the mature capsid structure (6) shown as an orange rope with side chains depicted as sticks. The residues conferring escape are shown (T242, G248, N252, and M250). Note the close proximity of T242 to T180 (corresponding to T182 in SIV). T180 also forms an N-capping box; in this case, TXXD(183) stabilizes helix 3 and D183 also stabilizes the N-terminal hairpin. Residues I256 and M228, at which compensatory mutations occur, are also shown as sticks.

ture (6, 31); green ribbon, CypA-bound structure (6, 14); cyan ribbon, CypA. Gray arrows indicate the observed conformational movements in the N-terminal hairpin, the CypA binding loop, and helix 6. Residue T242 is shown in magenta and drawn in stick representation. (b) Close-up of the TW10 epitope (magenta). The T(242)XXE(245) N-terminal cap for helix 6 is shown, with hydrogen bonds drawn as yellow dashes. Side chains (6) are drawn in stick representation. Hydrogen bonds between Trp-249, Glu-245, and the base of the CypA loop are shown together with Gly-248. (c) Ribbon representation as in panels a and b, with the mature capsid structure (6) shown as an orange rope with side chains depicted as sticks. The residues conferring escape are shown (T242, G248, N252, and M250). Note the close proximity of T242 to T180 (corresponding to T182 in SIV). T180 also forms an N-capping box; in this case, TXXD(183) stabilizes helix 3 and D183 also stabilizes the N-terminal hairpin. Residues I256 and M228, at which compensatory mutations occur, are also shown as sticks.

ture (6, 31); green ribbon, CypA-bound structure (6, 14); cyan ribbon, CypA. Gray arrows indicate the observed conformational movements in the N-terminal hairpin, the CypA binding loop, and helix 6. Residue T242 is shown in magenta and drawn in stick representation. (b) Close-up of the TW10 epitope (magenta). The T(242)XXE(245) N-terminal cap for helix 6 is shown, with hydrogen bonds drawn as yellow dashes. Side chains (6) are drawn in stick representation. Hydrogen bonds between Trp-249, Glu-245, and the base of the CypA loop are shown together with Gly-248. (c) Ribbon representation as in panels a and b, with the mature capsid structure (6) shown as an orange rope with side chains depicted as sticks. The residues conferring escape are shown (T242, G248, N252, and M250). Note the close proximity of T242 to T180 (corresponding to T182 in SIV). T180 also forms an N-capping box; in this case, TXXD(183) stabilizes helix 3 and D183 also stabilizes the N-terminal hairpin. Residues I256 and M228, at which compensatory mutations occur, are also shown as sticks.

ture (6, 31); green ribbon, CypA-bound structure (6, 14); cyan ribbon, CypA. Gray arrows indicate the observed conformational movements in the N-terminal hairpin, the CypA binding loop, and helix 6. Residue T242 is shown in magenta and drawn in stick representation. (b) Close-up of the TW10 epitope (magenta). The T(242)XXE(245) N-terminal cap for helix 6 is shown, with hydrogen bonds drawn as yellow dashes. Side chains (6) are drawn in stick representation. Hydrogen bonds between Trp-249, Glu-245, and the base of the CypA loop are shown together with Gly-248. (c) Ribbon representation as in panels a and b, with the mature capsid structure (6) shown as an orange rope with side chains depicted as sticks. The residues conferring escape are shown (T242, G248, N252, and M250). Note the close proximity of T242 to T180 (corresponding to T182 in SIV). T180 also forms an N-capping box; in this case, TXXD(183) stabilizes helix 3 and D183 also stabilizes the N-terminal hairpin. Residues I256 and M228, at which compensatory mutations occur, are also shown as sticks.

Gag residue	210	220	230	240	250	260
B consensus	AEWDR ^L LHPVH	AGPIAPGQMR	EPRGSDIAGT	TSTLQEQIGW	MTSNPP ^I IPVG	E
C consensus	AEWDR ^L LHPVH	AGPIAPGQMR	EPRGSDIAGT	TSTLQEQI ^A W	MT ^S SNPP ^V IPVG	D
T242N mutation	AEWDR ^L LHPV ^Q	AGPVAPGQMR	EPRGSDIAGT	T ^S N ^L LQEQI ^A W	MTSNPP ^V IPVG	D
A248X mutation	AEWDR ^L LHPVH	AGPIAPGQMR	EPRGSDIAGT	TSTLQEQI ^T W	MTSNPP ^I IPVG	D
M250I mutation	AEWDR ^L LHPVH	AGPIAPGQMR	EPRGSDIAGT	TSTLQEQI ^A W	^I T ^S SNPP ^I IPVG	D
S252N mutation	AEWDR ^L LHPVH	AGPIAPGQ ^L MR	EPRGSDIAGT	TSTLQEQI ^A W	MT ^S SNPP ^V IPVG	D

	Clade	B*57/5801-positive	B*57/5801-negative	All subjects
T242N/H219X*	B/C	(n=206) p=2.5x10 ⁻⁶ [47/106/1/52]†	(n=239) ns [0/4/26/209]	(n=445) p=9.4x10 ⁻⁸ [47/110/27/261]
A248X*/V256I	C	(n=126) p=0.00019 [20/0/65/21]	(n=132) p=0.0011 [14/2/51/65]	(n=258) p=3.1x10 ⁻⁷ [34/2/116/86]
M250I/S252G-V256I-D260E	C	(n=126) p=2.4x10 ⁻⁶ [8/5/6/107]	(n=132) p=3.2x10 ⁻⁸ [6/4/0/122]	(n=258) p=5.5x10 ⁻¹³ [14/9/6/229]
S252N/M228L	C	(n=126) p=1.5x10 ⁻⁹ [13/14/1/98]	(n=132) p=1.6x10 ⁻⁷ [17/20/5/90]	(n=258) p=8.4x10 ⁻¹⁶ [30/34/6/188]

FIG. 3. Polymorphisms within the Gag p24 N-terminal domain associated with TW10-linked mutations at Gag residues 242, 248, 250, and 252. * For H219X, X = Q in 71 cases, P in 2, and R in 1; for A248X, X = 20T, 5G, 3Q, 3N, 4D, and 1I. † Data for 2 by 2 tables is represented as [47/106/1/52], where 47 subjects had T242N and H219X, 106 subjects had T242N and H219, 1 subject had T242 and H219X, and 52 subjects had T242 and H219.

“Compensatory” and alternative escape mutations associated with TW10 escape. Escape within TW10 via T242N mutation and within CM9 via T180A mutation, with both epitopes associated with the control of viremia, is associated with additional variants that are hypothesized to compensate for the cost of the escape mutation (13, 24). Such “compensatory” mutations were first described in relation to a third p24 Gag epitope associated with successful control of HIV-1, the HLA-B27-KK10 HIV-1-specific epitope (20). We hypothesized that since the dominant TW10 escape mutation, T242N, exacts an in vitro fitness cost, alternative TW10 escape mutations would likewise reduce fitness and therefore require compensatory changes to be selected.

Additional TW10 escape mutations, in C clade infections only, were identified from the observation that a significantly larger number of B*5801-positive subjects have no escape mutation within TW10 than B*57-positive subjects (18/78 versus 1/48; $P = 0.001$). A flanking mutation downstream of the C terminus, either M250I or S252N, is associated with a lack of variation within TW10 ($P = 1.0 \times 10^{-5}$ and $P = 0.044$, respectively) (Fig. 3). The mechanism driving the acquisition of the M250I and S252N mutations is unknown and is the subject of a separate study. However, the association of these mutations with a lack of escape within TW10 suggests that these may represent processing escape mutations, as recently described for HIV infection (1, 9, 33).

To examine the possibility that the TW10 mutations at Gag residues 248, 250, and 252 might also select for compensatory mutations, associations between these polymorphisms and others within the capsid protein were sought (Fig. 3). For each of these, a strong association with a potential compensatory mutation(s) was identified (Fig. 3). For example, for B*57/5801-positive subjects, variation at Gag residue 248 in C clade infections was observed in association with variation at Val-256 in 20/20 cases, whereas wild-type Ala-248 was associated with variation at Val-256 in 65/106 subjects ($P = 0.0002$). Moreover, these associations persisted in B*57/5801-negative subjects,

both suggesting a lack of reversion following transmission and providing strong evidence for the interdependence of apparently minor sequence changes within this protein. For example, Ala-248 variation is also associated with Val-256 variation in B*57/5801-negative subjects ($P = 0.0011$); for all subjects, therefore, irrespective of HLA type, the association between variation at Ala-248 and that at Val-256 is strong ($P = 3.1 \times 10^{-7}$). These data suggest that evasion of the TW10 CTL response is severely limited by restrictions on sequence changes allowable within p24 Gag.

The one exception to this rule is the G248A mutation within TW10, which occurs at little or no cost to the virus: the G248A mutation arises commonly in B clade infections, persists upon transmission to B*57/5801-negative subjects (24), is not associated with a putative compensatory mutation, and actually increases infectivity (32). However, on its own, it is not an effective escape variant. The G248A change alone brings about a partial loss of recognition of the epitope, while the T242N mutation alone causes a greater loss of recognition, and the combination of the T242N and G248A mutations completely abrogates recognition at low peptide concentrations (24). In C clade infections, however, where Ala-248 is the consensus, the escape A248X mutation is relatively uncommon, arising only in association with the V256I mutation, as described above. An A248G mutation as an escape mutation in C clade infections is notably rare (Table 1), consistent with the evidence that the G248A mutation increases rather than decreases infectivity (32). These data suggest that this commonly arising G248A change in B clade infections arises at little or no cost to viral replicative capacity but is relatively ineffective as an escape variant except in company with the T242N mutation.

Structural analysis indicates that Gag residue 248 is on the side of helix 6 in proximity to the CypA binding loop. Indeed, when CypA is bound, Met-228 in the CypA binding loop packs against Gly-248. Thus, variants at Gag residue 248 are likely to have an effect on the packing of the CypA binding loop, although since Gag residue 248 is Ala in wild-type clade C, this

effect is apparently not deleterious. The importance of these finely balanced interactions is further emphasized by the observations that the V256I mutation is tightly linked with A248 variants in C clade infections and that the M228L mutation is similarly strongly associated with the S252N mutation (Fig. 2c and 3).

DISCUSSION

This study addresses one of the central conflicts in the engagement between HIV and the immune response, namely, the balance between the opposing forces driving mutational escape and those driving sequence conservation: this may be decisive in influencing outcomes from HIV-1 infection. HLA-B*57 and HLA-B*5801 are associated with effective control of HIV-1 (21), and a proposed mechanism to contribute to this instance of successful immune control (24) is that B*57/5801-restricted CTL target a conserved epitope, TW10, from which escape comes only at a cost to viral replicative capacity. This study demonstrates an *in vitro* fitness cost resulting from the T242N mutation. Alternative escape options for the virus are limited, given that all alternative sites of TW10 escape are associated with linked mutations, suggesting required functional compensation. The mechanisms for these associations between TW10 escape mutations and their linked polymorphisms are presently unknown. However, these structural data indicate the critical role of Thr-242 in nucleating and stabilizing helix 6 in the capsid protein and highlight the interdependence of key residues within TW10, helix 6, and the CypA loop to explain the observed inflexibility of sequence changes in this region. As with other epitopes associated with successful HIV/SIV control (4, 13, 14, 19), the capsid protein is a promising target for effective CTL, perhaps because of selection pressure against single escape mutations arising in the absence of linked compensatory changes.

Recent studies from the SIV macaque model of HIV infection have demonstrated the similar phenomenon of pyrrhic escape, that is, viral escape from a particular CTL specificity followed by immune control (26). However, it was noted from follow-up studies that escape mutation within a single capsid protein epitope, albeit occurring at a fitness cost, may not be sufficient to explain the subsequent immune control of immunodeficiency virus enjoyed by those macaques (22). In other words, HLA-B*57 and -B*5801-restricted CTL responses in addition to that to TW10 may be required to explain the successful control of HIV observed in persons expressing these HLA alleles.

The putative compensatory mutations that are described in this study also warrant further discussion. The associations between particular Gag capsid protein polymorphisms and the TW10-related escape mutations identified suggest a biological interdependence between the linked mutations. However, it is not known how this interdependence operates. Although the data presented have emphasized a potential structural role for these reciprocal changes, the compensatory mutations may operate via a wholly different mechanism. For example, the H219X mutation observed almost exclusively in association with the T242N mutation in B*57/5801-positive subjects (Fig. 3) (only 1 of 48 B*57/5801-positive subjects having the H219X mutation did not have the T242N mutation; $P = 2.5 \times 10^{-6}$)

may be selected as a means by which viral replicative capacity is restored to its original level, but in a way that is independent of the structural impact of the T242N substitution. Our own preliminary data (not shown) indicate that the introduction of the substitution H219Q increases the replicative capacity of the virus carrying the T242N mutation *in vitro*. This would be consistent with a recent paper demonstrating that H219Q and H219P mutations increase viral replicative capacity independent of any change at T242 (15). Similarly, under pressure from particular protease inhibitors, a necessary requirement for the replication competence of drug-resistant virus was the development of substitutions in Gag such as H219Q (16).

Furthermore, these data emphasize the predictable nature of escape mutations, prompting the hypothesis that prior vaccination with both wild-type virus and the anticipated escape mutants would limit viral escape options even further than in natural infection. Primary responses in individual subjects can be generated both to wild-type TW10 and to the escape forms (10). The absence of TW10 escape is associated with long-term control of HIV (27), so simultaneously shutting down all viable escape options may prove a highly successful strategy against HIV-1, if it can be implemented. The use of structural data to aid in identification of the limits of the capacity of the virus to evade potent early CTL responses thus forms a valuable contribution to vaccine design.

ACKNOWLEDGMENTS

This work was funded by the NIH (contracts NO1-A1-15422 and A146995-01A1) and the Wellcome Trust (A.L. and P.G.). J.M.-P. has a contract (99/3132) and J.G.P. has a BEFI fellowship (01/9067) from the Spanish Ministry of Health. B.W. is a Doris Duke Distinguished Clinical Science Professor, D.I.S. is an MRC research professor, and P.G. is an Elizabeth Glaser Pediatric AIDS Foundation scientist.

We thank Robert Esnouf and Paul Klenerman for discussions.

REFERENCES

- Allen, T. M., M. Altfeld, X. G. Yu, K. M. O'Sullivan, M. Lichterfeld, S. Le Gall, M. John, B. R. Mothe, P. K. Lee, E. T. Kalife, D. E. Cohen, K. A. Freedberg, D. A. Strick, M. N. Johnston, A. Sette, E. S. Rosenberg, S. A. Mallal, P. J. R. Goulder, C. Brander, and B. D. Walker. 2004. Selection, transmission, and reversion of an antigen-processing CTL escape mutation in HIV-1 infection. *J. Virol.* **78**:7069–7078.
- Altfeld, M., M. M. Addo, E. S. Rosenberg, F. M. Hecht, P. K. Lee, M. Vogel, Yu, X. G., et al. 2003. Influence of HLA-B57 on clinical presentation and viral control during acute HIV-1 infection. *AIDS* **17**:2581–2591.
- Aurora, R., and G. D. Rose. 1998. Helix capping. *Protein Sci.* **7**:21–38.
- Barouch, D. H., J. Kunstman, M. J. Kuroda, J. E. Schmitz, et al. 2002. Eventual AIDS vaccine failure in a rhesus monkey by viral escape from CTL. *Nature* **415**:335–339.
- Barouch, D. H., J. Powers, D. M. Truitt, M. G. Kishko, J. C. Arthur, F. W. Peyerl, M. J. Kuroda, et al. 2005. Dynamic immune responses maintain CTL epitope mutations in transmitted SIV variants. *Nat. Immunol.* **6**:232–234.
- Berman, H. M., J. Westbrook, Z. Feng, G. Gilliland, T. N. Bhat, H. Weissig, I. N. Shindyalov, and P. E. Bourne. 2000. The Protein Data Bank. *Nucleic Acids Res.* **28**:235–242.
- Berthet-Colominas, C., S. Monaco, A. Novelli, G. Sibai, F. Mallet, and S. Cusack. 1999. Head-to-tail dimers and interdomain flexibility revealed by the crystal structure of HIV-1 capsid protein (p24) complexed with a monoclonal antibody Fab. *EMBO J.* **18**:1124–1136.
- Braaten, D., E. K. Franke, and J. Luban. 1996. Cyclophilin A is required for an early step in the life cycle of HIV-1 before the initiation of reverse transcription. *J. Virol.* **70**:3551–3560.
- Draenert, R., S. Le Gall, K. J. Pfafferoth, et al. 2004. Immune selection for altered antigen processing leads to cytotoxic T lymphocyte escape in chronic HIV-1 infection. *J. Exp. Med.* **199**:905–915.
- Feeney, M. E., Y. Tang, K. Pfafferoth, K. A. Roosevelt, et al. 2005. HIV-1 viral escape in infancy followed by emergence of a variant-specific CTL response. *J. Immunol.* **174**:7524–7530.
- Fernandez, C. S., I. Stratov, R. De Rose, K. Walsh, C. J. Dale, M. Z. Smith, M. B. Agy, S.-L. Hu, K. Krebs, D. I. Watkins, D. H. O'Connor, M. P.

- Davenport, and S. J. Kent. 2005. Rapid viral escape at an immunodominant simian-human immunodeficiency virus cytotoxic T-lymphocyte epitope exacts a dramatic fitness cost. *J. Virol.* **79**:5721–5731.
12. Friedrich, T. C., E. J. Dodds, L. J. Yant, L. Vojnov, R. Rudersdorf, C. Cullen, D. T. Evans, R. C. Desrosiers, et al. 2004. Reversion of CTL escape-variant immunodeficiency viruses in vivo. *Nat. Med.* **10**:275–281.
 13. Friedrich, T. C., C. A. Frye, L. J. Yant, D. H. O'Connor, N. A. Kriewaldt, M. Benson, L. Vojnov, E. J. Dodds, C. Cullen, R. Rudersdorf, A. L. Hughes, N. Wilson, and D. I. Watkins. 2004. Extraepitopic compensatory substitutions partially restore fitness to SIV variants that escape from an immunodominant CTL response. *J. Virol.* **78**:2581–2585.
 14. Gamble, T., F. Vajdos, S. Yoo, D. WorthyLake, M. Hoesweart, W. I. Sunquist, and C. P. Hill. 1996. Crystal structure of human cyclophilin A bound to the amino-terminal domain of HIV-1 capsid. *Cell* **87**:1285–1294.
 15. Gatanaga, H., D. Das, Y. Suzuki, D. D. Yeh, K. A. Hussain, A. Ghosh, and H. Mitsuya. 2006. Altered HIV-1 Gag protein interactions with cyclophilin A (CypA) upon the acquisition of H219Q and H219P substitutions in the CypA binding loop. *J. Biol. Chem.* **281**:1241–1250.
 16. Gatanaga, H., Y. Suzuki, H. Tsang, K. Yoshimura, M. F. Kavlick, K. Nagashima, R. J. Gorelick, S. Mardy, C. Tang, M. F. Summers, and H. Mitsuya. 2002. Amino acid substitutions in Gag protein at noncleavage sites are indispensable for the development of a high multitude of HIV-1 resistance against protease inhibitors. *J. Biol. Chem.* **277**:5952–5961.
 17. Gibbs, J. S., D. A. Regier, and R. C. Desrosiers. 1994. Construction and in vitro properties of HIV-1 mutants with deletions in “nonessential” genes. *AIDS Res. Hum. Retrovir.* **10**:343–350.
 18. Goulder, P. J. R., and D. I. Watkins. 2004. HIV and SIV CTL escape: implications for vaccine design. *Nat. Rev. Immunol.* **4**:630–640.
 19. Goulder, P. J. R., R. E. Phillips, R. A. Colbert, S. McAdam, et al. 1997. Late escape from an immunodominant CTL response associated with progression to AIDS. *Nat. Med.* **3**:212–217.
 20. Kelleher, A. D., C. Long, E. C. Holmes, et al. 2001. Clustered mutations in HIV-1 gag are consistently required for escape from HLA-B27-restricted CTL responses. *J. Exp. Med.* **193**:375–386.
 21. Kiepiela, P., A. J. Leslie, I. Honeyborne, D. Ramduth, C. Thobakgale, S. Chetty, P. Rathnavalu, C. B. Moore, et al. 2004. Dominant influence of HLA-B in mediating the potential coevolution of HIV and HLA. *Nature* **432**:769–775.
 22. Kobayashi, M., H. Igarashi, A. Taskeda, M. Kato, and T. Matano. 2005. Reversion in vitro after inoculation of a molecular proviral DNA clone of simian immunodeficiency virus with a cytotoxic T lymphocyte escape mutation. *J. Virol.* **79**:11529–11532.
 23. Koenig, S., A. J. Conley, Y. A. Brewah, et al. 1995. Transfer of HIV-1-specific CTL to an AIDS patient leads to selection for mutant HIV variants and subsequent disease progression. *Nat. Med.* **1**:330–336.
 24. Leslie, A. J., K. J. Pfafferoth, P. Chetty, R. Draenert, M. M. Addo, M. Feeney, Y. Tang, et al. 2004. HIV evolution: CTL escape mutation and reversion after transmission. *Nat. Med.* **10**:282–289.
 25. Leslie, A. J., D. Kavanagh, I. Honeyborne, et al. 2005. Transmission and accumulation of CTL escape variants drives negative associations between HIV polymorphisms and HLA. *J. Exp. Med.* **201**:891–902.
 26. Matano, T., M. Kobayashi, H. A. Igarashi, et al. 2004. CTL-based control of SIV replication in a preclinical AIDS vaccine trial. *J. Exp. Med.* **199**:1709–1718.
 27. Migueles, S. A., A. C. Laborico, H. Imamichi, W. L. Shupert, C. Royce, M. McLaughlin, L. Ehler, J. Metcalf, S. Liu, C. W. Hallahan, and M. Connors. 2003. The differential ability of HLA B*5701⁺ long-term nonprogressors and progressors to restrict human immunodeficiency virus replication is not caused by loss of recognition of autologous viral gag sequences. *J. Virol.* **77**:6889–6898.
 28. Momany, C., L. C. Kovari, A. J. Prongay, et al. 1996. Crystal structure of dimeric HIV-1 capsid protein. *Nat. Struct. Biol.* **3**:763–770.
 29. Moore, C. B., M. John, I. R. James, F. T. Christiansen, C. S. Witt, and S. A. Mallal. 2002. Evidence of HIV-1 adaptation to HLA-restricted immune responses at a population level. *Science* **296**:1439–1443.
 30. Pao, D., U. Andradý, J. Clarke, G. Dean, S. Drake, et al. 2004. Long-term persistence of primary genotypic resistance after HIV-1 seroconversion. *J. Acquir. Immune Defic. Syndr.* **37**:1570–1573.
 31. Tang, C., Y. Ndassa, and M. F. Summers. 2002. Structure of the N-terminal 283-residue fragment of the immature HIV-1 Gag polyprotein. *Nat. Struct. Biol.* **9**:537–543.
 32. von Schwedler, U., K. M. Stray, J. E. Garrus, and W. I. Sundquist. 2003. Functional surfaces of the human immunodeficiency virus type 1 capsid protein. *J. Virol.* **77**:5439–5450.
 33. Yokomaku, Y., H. Miura, H. Tomiyama, A. Kawana-Tachikawa, M. Takiguchi, A. Kojima, Y. Nagai, A. Iwamoto, Z. Matsuda, and K. Ariyoshi. 2004. Impaired processing and presentation of cytotoxic-T-lymphocyte (CTL) epitopes are major escape mechanisms from CTL immune pressure in human immunodeficiency virus type 1 infection. *J. Virol.* **78**:1324–1332.
 34. Yusim, K., C. Kesmir, B. Gaschen, M. M. Addo, M. Altfeld, S. Brunak, A. Chigaev, V. Detours, and B. T. Korber. 2002. Clustering patterns of cytotoxic T-lymphocyte epitopes in human immunodeficiency virus type 1 (HIV-1) proteins reveal imprints of immune evasion on HIV-1 global variation. *J. Virol.* **76**:8757–8768.